Multichromophoric Sensitizers Based on Squaraine for NiO Based Dye-Sensitized Solar Cells

ARTICLE *in* THE JOURNAL OF PHYSICAL CHEMISTRY C · DECEMBER 2013

Impact Factor: 4.77 · DOI: 10.1021/jp408900x

8 AUTHORS, INCLUDING:

Loïc Le Pleux
University of Basel
19 PUBLICATIONS **890** CITATIONS

SEE PROFILE

Leif Hammarström
Uppsala University
162 PUBLICATIONS **6,477** CITATIONS

SEE PROFILE

THE JOURNAL OF PHYSICAL CHEMISTRY C

Article

pubs.acs.org/JPCC

Multichromophoric Sensitizers Based on Squaraine for NiO Based Dye-Sensitized Solar Cells

Julien Warnan,[†] James Gardner,[‡] Loïc Le Pleux,[†] Jonas Petersson,[‡] Yann Pellegrin,[†] Errol Blart,[†] Leif Hammarström,*[,‡] and Fabrice Odobel*[,†]

[†]Université LUNAM, Université de Nantes, CNRS, Chimie et Interdisciplinarité: Synthèse, Analyse, Modélisation (CEISAM), UMR 6230, 2 rue de la Houssinière, 44322 Nantes cedex 3, France

[‡]Department of Chemistry − Ångström Laboratory, Uppsala University, Box 523, Uppsala, SE75120 Sweden

Supporting Information

ABSTRACT: Three sensitizers were synthesized and utilized as panchromatic dyes for nanocrystalline NiO films: an iodo-squaraine (SQ), a squaraine-perylene monoimide (SQ-PMI) dyad, and a squaraine-perylene monoimide-naphthalene diimide (SQ-PMI-NDI) triad. Photophysical and photovoltaic studies showed that hole injection into the NiO valence band from the SQ excited state is ultrafast, but also that subsequent recombination is very rapid, preventing SQ from being an efficient sensitizer for photovoltaic purposes. The introduction of a second light harvesting unit (PMI) and a terminal electron acceptor (NDI) significantly improved the photovoltaic performances of the system. Irrespective of which light harvesting unit was photoexcited in NiO/SQ-PMI and NiO/SQ-PMI-NDI, intramolecular charge separation leading to SQ^+ and PMI^- or NDI^- is the main excited state deactivation process. Intramolecular charge separation occurred in spite of the favorable conditions for energy transfer to the SQ unit. Subsequent hole injection from SQ^+ into NiO was in competition with intramolecular recombination, which may have significantly decreased the overall photovoltaic performances. The control of this side-reaction is therefore crucial for the successful design of multichromophoric systems for dye-sensitized solar cells (DSSCs). The quantum yield of $NiO^{(+)}/SQ\text{-}PMI\text{-}NDI^-$ after 50 ns is higher than that of $NiO^{(+)}/SQ\text{-}PMI^-$, and much higher than that of $NiO^{(+)}/SQ^-$; intramolecular recombination was slowed down by the localization of the electron further away from the SQ^+ hole and consequently from NiO^+. The three sensitizers were tested in NiO based DSSC devices using either the conventional triiodide/iodide electrolyte or a $cobalt^{III/II}$(4,4′-di-*tert*-butyl-2,2′-bipyridine)$_3$ electrolyte. The photoconversion efficiencies steadily increased in the following order: SQ < SQ-PMI < PMI-NDI ≪ SQ-PMI-NDI. The multichromophoric sensitizers had broader absorption spectra, more long-lived charge separation, and better photovoltaic performance than single unit chromophores. This indicates that bichromophoric systems, ones in which the antenna serves both as electron acceptor and photon harvester, are realistic sensitizers to boost photovoltaic performances. These findings are important for engineering new panchromatic and more efficient sensitizers for p-type DSSCs.

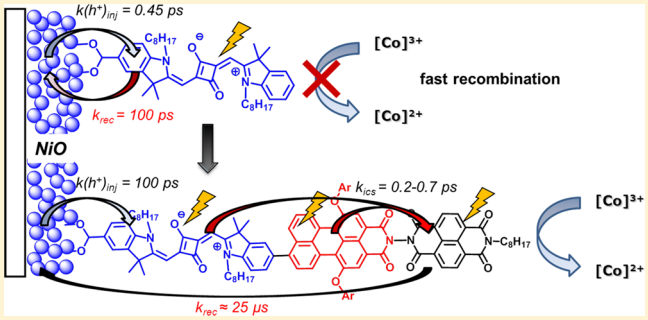

INTRODUCTION

The rational design of efficient photocathodes based on the sensitization of a p-type semiconductor (p-SC), such as nickel oxide (NiO), is an important, complementary task for matching the well-mastered TiO_2 photoanode to develop tandem dye-sensitized solar cells (DSSCs)[1−3] or photoelectrocatalytic systems for solar fuels production.[4,5] There are few studies devoted to the sensitization of p-type dye-sensitized solar cells, and these are more recent than those dedicated to the conventional Grätzel cells; however, there has been an explosion of interest in this area for the past 3 years.[6,7] For most simple sensitizers, the hole injection into the valence band (VB) of NiO is generally ultrafast (predominantly less than 1 ps) but also charge recombination is rapid (predominantly in less than 1 ns for simple dyes).[8−13] As a result, the subsequent shift of the electron residing on the photoreduced sensitizer to a redox mediator in solution is inefficient and this significantly limits the overall performances of the DSSCs.

So far, the most effective strategy to slow down the charge recombination reaction, and one which permits engineering the most efficient sensitizers, consists of a bicomposite system composed of a sensitizer connected to an electron acceptor.[3,6,11,13−15] The two charges are separated over a large distance, which results in an ion pair lifetime that is greatly enhanced and provides an expanded time frame for bimolecular electron transfer (i.e., with the redox mediator). On the other hand, multichromophoric dyes have proven particularly useful to broaden the absorption cross-section of a given sensitizer for

Received: September 5, 2013
Revised: December 11, 2013
Published: December 12, 2013

n-type systems, and consequently improving the photoconversion efficiency of a DSSC.[16−22] In these multichromophoric systems, the photons are collected by several dyes having complementary absorption spectra and the incident light energy is directed toward a single dye by energy transfer processes. The latter dye is linked to the SC surface and decays by injecting charges into the SC. Natural photosynthetic organisms have used this strategy for billions of years to maximize the absorption cross-section of sunlight by the photosynthetic reaction center. This is achieved via a large collection of different pigments located inside light harvesting antennae.[23,24]

In 2005, we reported the potential interest of incorporating light harvesting antennae into DSSCs.[25] We and others have since then prepared several elegant multichromophoric arrays highlighting the pertinence of the strategy for improving the photoconversion efficiency of Grätzel cells.[16−21] In this study, we wish to extend this concept to p-type dye-sensitized solar cells and furthermore to explore the possibility to use antennae not only as light harvesters, but also as a secondary electron acceptor to electronically and geometrically decouple the electron residing on the dye from the hole in the VB of NiO, thus to eventually enhance the lifetime of the photoreduced dye (Scheme 1).

To test the validity of such a concept, we prepared a dyad SQ-PMI and a triad SQ-PMI-NDI in which the sensitizer is a squaraine (SQ) and the antenna is a perylene monoimide (PMI) or a PMI-naphtalene diimide dyad (PMI-NDI) (Chart 1). Squaraine derivatives have been extensively used as dyes in classical (n-type) Grätzel cells[26−28] but they have rarely been used as sensitizers for NiO.[29] The very high extinction coefficient of SQ in the low energy region of the visible spectrum makeing it an appealing dye to test on NiO cathodes and particularly as energy sink component into an energy cascade multichromophoric system. The PMI chromophore is a strongly absorbing dye exhibiting a higher lying excited-state than SQ and is also a quite good electron acceptor. In the triad SQ-PMI-NDI, we searched to combine the high red-light harvesting property of the squaraine with the efficient PMI-NDI system reported before.[3,9,14] As shown below, in these two systems, there is an energy gradient along the assembly to funnel the photonic energy to the squaraine and to move the electron from NiO to the extremity of the system (PMI in the dyad and NDI in the triad). The synthesis, photophysical characterization by ultrafast transient absorption spectroscopy, and the photovoltaic properties of these new dyes in DSSCs are reported herein. In the dyad and triad, we found, contrary to our expectations, that intramolecular charge separation dominated over energy transfer and interfacial charge separation in the primary reaction steps. Nevertheless, this also proved to be a viable route to full charge separation, with an electron localized on the antenna spatially separated from the hole in NiO. The results validate the multichoromophoric design principle, wherein light harvesting and charge transfer are achieved within a single molecule, and show that multichromophoric sensitizers may lead to efficient NiO photocathodes.

Scheme 1. Expected Operation Principle of a Bichromophoric System in Which the Antenna Plays the Dual Role of a Light Harvester and of a Secondary Electron Acceptor[a]

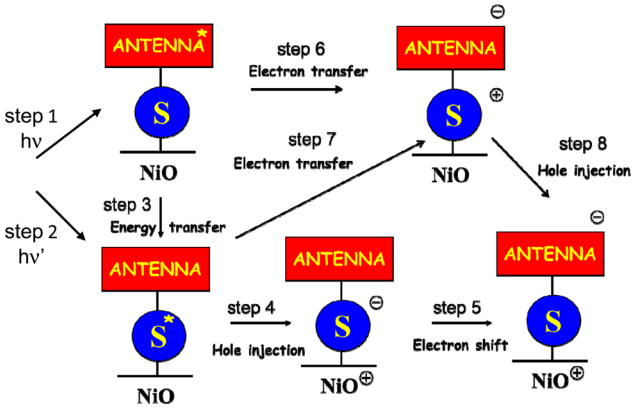

[a]Light absorption by the antenna unit ($h\nu$, step 1) followed by energy transfer (step 3), or direct excitation of the sensitizer ($h\nu'$, step 2), may lead to hole injection into NiO (step 4). This may be followed by an electron shift (step 5) from the reduced sensitizer (S^-) to the antenna, thus localizing the electron further from the $NiO^{(+)}$ hole. Alternatively (upper pathway in Scheme 1), intramolecular charge separation from the excited antenna (step 6) or sensitizer (step 7) may occur, followed by hole injection into NiO (step 8). The upper and lower pathways of Scheme 1 result in the same state with a reduced antenna and a hole in NiO. Overall, with a suitable bichromophoric system, an amplification of the light capture (dual absorber) and an increase of the charge separated state lifetime (extended distance between the charges) could be achieved.

Synthesis of the Compounds. The key reaction for the synthesis of the dyad SQ-PMI and of the triad SQ-PMI-NDI relies on a Suzuki-Miyaura cross-coupling between the known iodo-squaraine (SQ)[20] and the boronate of PMI (**3**) or of the dyad PMI-NDI (**4**). The latter were prepared from the corresponding bromo derivative (**1** or **2**) by palladium catalyzed insertion of bis(pinacolato)diboron (Scheme 2).[30,31] While the resulting pinacol boronic ester **3** was successfully purified on silica gel column chromatography in good yield (76%), attempts to purify the more polar compound **4** led to degradation, resulting probably from the hydrolysis of the boronic ester. As a result, the crude reaction mixture of **4** was washed, quickly filtered on a silica plug to remove residual inorganic and polar compounds and eventually engaged in the final palladium cross-coupling with SQ. Thus, the linkage between the squaraine and the perylene was realized by Suzuki coupling of SQ and **3** or **4** in toluene and methanol with tetrakispalladiumtriphenylphosphine as catalyst and hydrated barium hydroxide as a base. The crude reaction products were purified on silica gel to furnish SQ-PMI and SQ-PMI-NDI in 69% and 15% (on two steps) yield respectively.

Absorption Spectra. The absorption spectra of the sensitizers recorded in solution and on NiO electrodes are illustrated in Figures 1 and 2, respectively. The naphthalene diimide absorbing below 400 nm, the squaraine ($\lambda_{max} \approx 660$ nm), and the perylene monoimide ($\lambda_{max} \approx 530$ nm) are therefore the two visible light harvesting chromophores of the systems. The two latter dyes exhibit $\pi-\pi^*$ transitions, and they display complementary absorption bands that cover a broad spectral window between 450 and 700 nm, enabling a larger photon harvesting cross section than single chromophore systems (SQ or PMI). Interestingly, the maximum absorption wavelength of the squaraine is red-shifted and broadened in the dyad SQ-PMI and in the triad SQ-PMI-NDI relative to that in the reference SQ suggesting a significant electronic interaction between SQ and PMI. The broadening is tentatively assigned to

dx.doi.org/10.1021/jp408900x | J. Phys. Chem. C 2014, 118, 103−113

Chart 1. Structures of the Squaraine Compounds Described in This Study

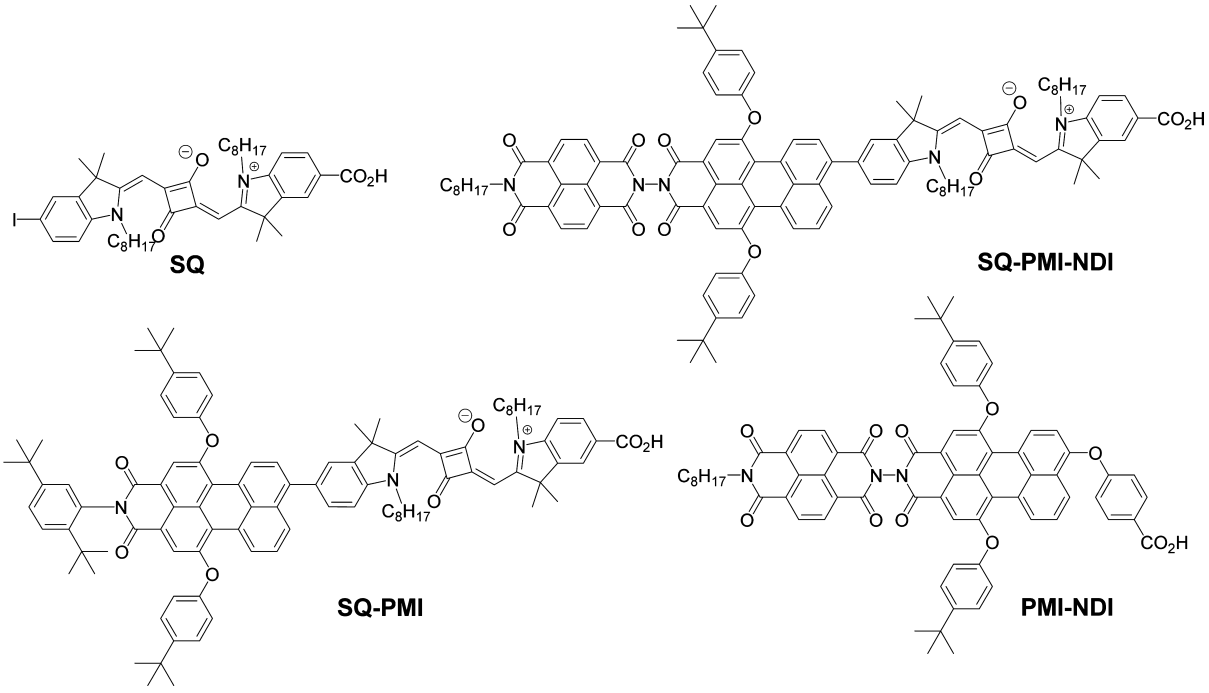

Scheme 2. Synthesis of Dyad PMI-SQ and Triad NDI-PMI-SQ[a]

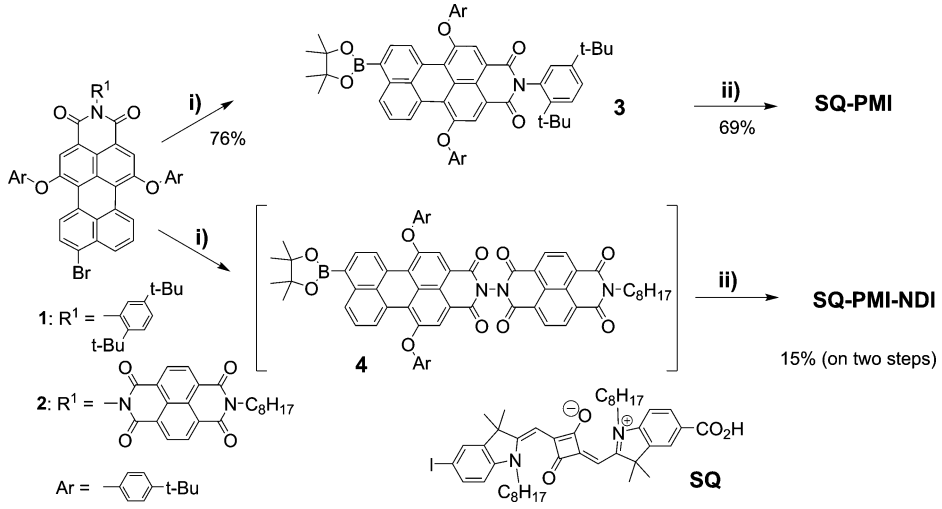

[a]Reagents and conditions: (i) bis(pinacolato)diboron, $Pd(dppf)Cl_2$, AcOK,1,4-dioxane, 70 °C, 16 h; (ii) SQ, $Pd(PPh_3)_4$, $Ba(OH)_2 \cdot 8H_2O$, toluene/MeOH, 80 °C, 2.5 h.

rotational freedom giving a distribution of angles between the SQ and PMI π-systems. Upon chemisorption of the dyes on NiO electrodes, the SQ exhibits two intense absorption bands (Figure 2). In spite of the presence of cheno-deoxycholic acid as coadsorbate, the higher energy absorption band (around 620 nm) suggest the formation of H-type aggregates[38] which seem to progressively break apart as we pass from SQ, SQ-PMI, and SQ-PMI-NDI. We note that the NDI transition (around 380 nm) is more intense on NiO than in solution. This is certainly due to the overlapping with the intrinsic NiO absorbance, which is difficult to accurately remove in this region.

Free Energy of the Photoinduced and Electron Transfer Reactions. Several photoinduced energy and electron transfer processes can be envisioned in these multichromophoric systems. These processes and the states involved are summarized in Scheme 3; calculations of the corresponding driving forces are given in the Supporting Information. The electron transfer driving forces within the dyad and triad molecules were calculated from the redox potentials and from singlet excited-state energy levels (E_{00}) determined from the individual subunits (Table 1). This was done instead of using the actual molecules because the dyad and triad are nonfluorescent and relatively unstable in solution when exposed to the sunlight. However, upon binding on NiO, the stability of the dyes is instead high, presumably because interfacial charge separation outcompetes degradation pathways.

One possible pathway from the initially excited chromophore is energy transfer (EnT) toward the SQ subunit, which then leads to hole injection (hinj) into NiO and a following electron

dx.doi.org/10.1021/jp408900x | J. Phys. Chem. C 2014, 118, 103−113

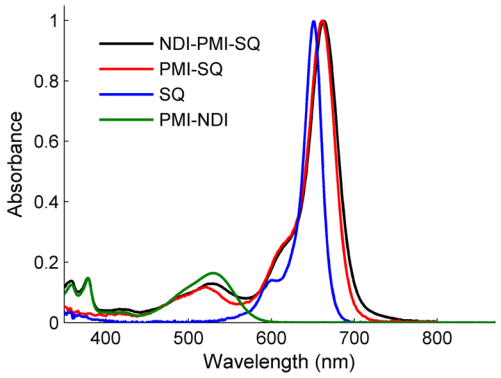

Figure 1. Overlay of the normalized absorption spectra of SQ, SQ-PMI, PMI-NDI, and SQ-PMI-NDI recorded in dichloromethane solution.

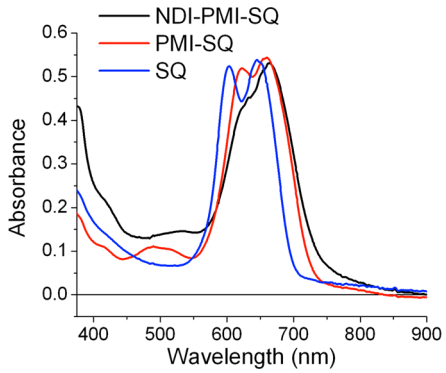

Figure 2. Absorption spectra of squaraine-based sensitizers recorded on mesoporous NiO films (~1 μm thick) and corrected for the absorbance from NiO and FTO glass.

shift (esh) from the SQ toward the NDI. All of these processes are indeed significantly exergonic and the molecular design of the dyad and triad thus fulfills the thermodynamic criteria to work as an antenna. Competing with this reaction pathway is the intramolecular electron transfer (iet) and internal charge separation (ics). These may, however, also lead to the desired hole injection (c.f. Scheme 1). The only reactions to be avoided are the charge recombination reactions to the ground state (cr, icr), which all have significant exergonicities.

Nanosecond-Transient Absorption Experiments. The sensitized NiO samples were investigated by time-resolved laser spectroscopy (see the Supporting Information). On a ns–μs time scale after excitation with a 10 ns laser pulse there are only small transient absorption changes observed for the NiO/SQ sample (Figure 3). The formation of the SQ^- radical should result in an absorption around 480 nm and a ground state bleach in the 600–700 nm region,[32] which were indeed observed. However, the small signals show that the yield of interfacial charge separation surviving on the 50 ns time scale was low. In contrast, the NiO/SQ-PMI and NiO/SQ-PMI-NDI samples show much stronger transient spectral features of the reduced dyes at 50 ns after excitation (Figure 3). The former sample displays peaks around 650 and 730 nm as well as a bleach around 500 nm, which can be attributed to the formation of the reduced PMI^- unit and concomitant PMI ground state bleach.[14,33,34] The triad sample instead shows one strong band with a maximum around 480 nm, and a double-peak feature at 600–700 nm, with a bleach around 730 nm. The 480 nm band, with a smaller peak at 605 nm, is

Scheme 3. Approximate State Energy and Reaction Scheme for the Relevant States Involved in the Deactivation Processes in SQ-PMI-NDI on NiO[a]

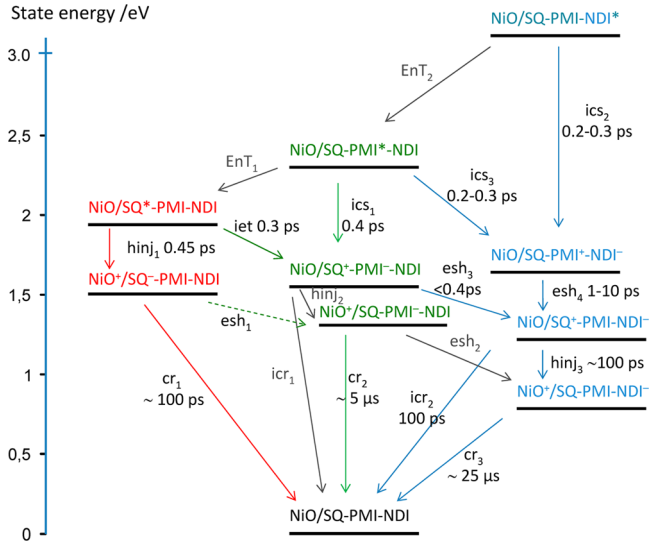

[a]The energies are calculated from electrochemical data and spectroscopic 0,0-energies. Reaction lifetimes are given for the observed processes (coloured arrows); esh_1 is implicated but not observed. All the interfacial charge transfer reactions are highly nonexponential, and the given lifetime represents only an average order of magnitude estimate. There is no evidence for excitation energy transfer between the molecular units, but this cannot be excluded as a minor process in parallel to charge separation. EnT = energy transfer; ics = intramolecular charge separation; esh = electron shift; iet = intramolecular electron transfer; hinj = hole injection in NiO; cr = charge recombination; icr = intramoelcular charge recombination. For more details of the legend, see the Supporting Information.

Table 1. Redox Potentials and Singlet Excited-State Energies of the Components of the Dyad and Triad[a]

compd	$E_{00}(^1S^*)$, eV[d]	$E_{1/2}(S^+/S)$, V	$E_{1/2}(S/S^-)$, V	$E_{1/2}(S^+/S^*)$, V[e]	$E_{1/2}(S^*/S^-)$, V[f]
SQ	1.90	0.61	−1.21	−1.29	0.69
PMI[b]	2.24	1.19	−1.01	−1.05	1.23
NDI[c]	3.10	>1.6 V	−0.51		2.59

[a]All potentials are given versus saturated calomel electrode (SCE). [b]Data taken from ref 14. [c]Data taken from PMI-NDI in ref 9. [d]Calculated with the equation $E_{00}(^1S^*) = 1240/\lambda_{inter}(nm)$; λ_{inter} = wavelength at the intersection of the absorption and emission spectra. [e]Calculated with the equation $E_{1/2}(S^+/S^*) = E_{1/2}(S^+/S) - E_{00}(^1S^*)$. [f]Calculated with the equation $E_{1/2}(S^*/S^-) = E_{1/2}(S/S^-) + E_{00}(^1S^*)$.

characteristic for the NDI^- radical.[33] Most of the features in the 600–730 nm region may be explained by a blue shift of the SQ ground state absorption. The shift of the ground state spectrum can either be a Stark-shift due the electric field of the interfacial charge separation, or a change in intramolecular interaction between the NDI and SQ units when the NDI is reduced; compare the red-shift of the dyad and triad SQ ground state spectra relative to that for SQ. This is discussed further below.

The yield of charge separation after 50 ns was an order of magnitude larger in the triad than in the dyad; there is a three times larger signal from $NDI^{\bullet-}$ in the triad than from PMI^- in the dyad, although the peak extinction coefficient of PMI^- is three times larger than that for $NDI^{\bullet-}$.[33] Interestingly, the yield

dx.doi.org/10.1021/jp408900x | J. Phys. Chem. C 2014, 118, 103–113

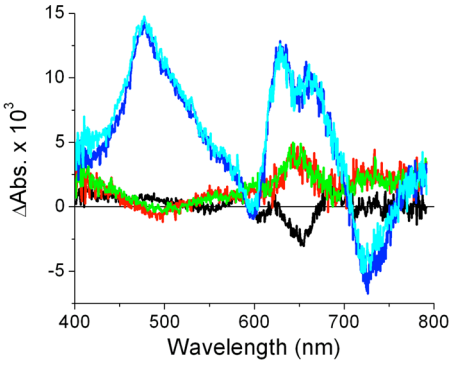

Figure 3. Transient absorption spectra 50 ns after excitation with a 10 ns laser pulse of the NiO films sensitized with SQ (black = 2 mJ 655 nm excitation), SQ-PMI (green = 3 mJ 520 nm excitation, red = 2 mJ 655 nm excitation), and SQ-PMI-NDI (light blue = 3 mJ 520 nm excitation, dark blue = 2 mJ 655 nm excitation); the samples had 0.1 M $LiClO_4$, but no redox couple in the propylene carbonate solvent.

was larger with excitation of the PMI unit at 520 nm than with excitation of the SQ unit at 655 nm, as the transient signal at 50 ns showed no significant difference although the absorbance at 655 nm was around 0.5 and that at 520 nm only 0.1−0.15. This reveals that the charge separation pathways are not the same, because the branched ratio depends on which unit is initially excited. This is further elucidated below by ultrafast transient absorption experiments on the femtosecond and picosecond time scale.

The decay of the transient signals was monitored up to 10 and 350 μs, respectively, for NiO/SQ-PMI and NiO/SQ-PMI-NDI (Figure 4). The decay is attributed to recombination with the $NiO^{(+)}$ holes. A fit to the data on this time scale using the Kohlrausch−William−Watts equation (eq 1) gave an average lifetime $\langle\tau\rangle$ = 26 μs for the triad and $\langle\tau\rangle$ = 5 μs for the dyad. Although some recombination may occur also on shorter time scales than observed in this experimental window (see below), this illustrates that electron transfer from the attached dye to appended acceptor groups substantially slows down recombination with $NiO^{(+)}$ compared to the typical <1 ns time scale observed for a range of different dyes on NiO.[3,9,10,14,34−37]

$$\Delta\mathrm{Abs} = \Delta A_0 e^{-(t/\tau)^{\beta}} \quad (1)$$

We note that the transient absorption traces monitored at 625 nm, due to the shift of the SQ ground state spectrum, decay faster than those monitoring the NDI^{-} absorption at 475 nm; see Figure S6 in the Supporting Information. This shows that the ground state shift is not proportional to the concentration of NDI^{-}. Also, the shift is much smaller for the NiO/SQ-PMI sample where the reduced species is directly attached to SQ, but where the concentration of charge separated species is ca. 10-fold lower. We therefore assign the ground state shift to a Stark effect.

Femtosecond-Transient Absorption Experiments. Interpretation of the ultrafast transient absorption data was complicated by several factors: (1) the SQ ground state extinction coefficient is very large, so that ground state bleach dominates and covers the other signals; (2) the strong electronic coupling between the units perturbs the SQ spectrum (Figures 1 and 2) and may also lead to delocalized excited states, which questions the distinction of weakly coupled but individual SQ, PMI and NDI subunits; (3) the ultrafast rate of the initial electron transfer processes (see below) that presumably occurs in parallel to molecular and solvent relaxation; (4) the possibility of different intramolecular and interfacial energy transfer and charge separation processes occurring simultaneously; (5) aggregate formation (cf. Figures 1 and 2); and (6) reference experiments in solution were not possible because of rapid sample degradation under those conditions. Nevertheless, we could elucidate the most important processes, as described below.

All samples were excited with 120 fs laser pulses at either 640−670, 523, or 400 nm, exciting selectively the SQ, PMI, or NDI unit, respectively (note that absorption of SQ 400−530 nm is negligible, see Figure 1). Transient absorption spectra (chirp corrected) at different times are shown in Figures 5−9. A global fit to the data was made using eq 2:

$$\Delta\mathrm{Abs} = c_1 \exp(-t/\tau_1) + c_2 \exp(-t/\tau_2) + c_3 \exp(-t/\tau_3) + c_4 \quad (2)$$

The pre-exponential factors c_1−c_4 obtained were used to construct decay associated spectra (DAS) that show the spectral changes associated with each lifetime component. Full experimental details are given in the Supporting Information.

NiO/SQ. The transient absorption spectrum at 0.1 ps after excitation with a 120 fs laser pulse at 647 nm can be attributed to the lowest singlet excited state of the squaraine, with a strong and broad band in the 400−570 nm range, a ground-state bleach, and stimulated emission (Figure 5). The spectrum evolves rapidly: the stimulated emission around 690 nm

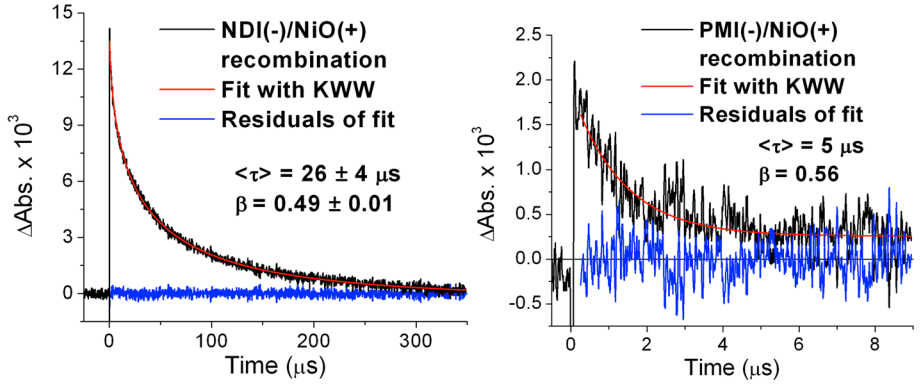

Figure 4. Transient absorption trace after 10 ns laser excitation at 655 nm: (left) NiO/SQ-PMI-NDI monitored at 480 nm; (right) NiO/SQ-PMI monitored at 650 nm; samples as in Figure 3.

dx.doi.org/10.1021/jp408900x | J. Phys. Chem. C 2014, 118, 103−113

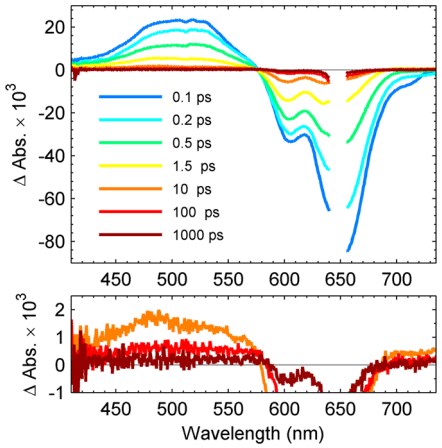

Figure 5. Transient absorption spectra of NiO/SQ excited at 647 nm. Lower panel shows the spectra after 10, 100, and 1000 ps on an expanded scale. Samples: as in Figure 3.

disappears with a lifetime of 0.45 ps and the signal turns into a weak net absorption (Figure S1, Supporting Information). The disappearance of the other signals is somewhat slower, but after 10 ps the spectrum shows a broad absorption band around 480 nm in addition to a ground state bleach. These spectral features are expected for the reduced SQ^- species,[32] although the signals are small compared to those from the initial excited state. A fit to eq 2 gave the lifetime components in Table 2. With help of the DAS (Figure S2, Supporting Information), it is clear that the τ_3 component of 53 ps shows the 480 nm band, which we therefore attribute to the decay of the SQ^- via recombination with $NiO^{(+)}$. The DAS for the fastest component τ_1 = 0.45 ps shows the disappearance of the stimulated emission: a 650 nm maximum and a 700 nm shoulder; this is in good agreement with the fluorescence spectrum of SQ in solution. It can therefore be attributed to interfacial electron transfer from the excited SQ* state to generate $NiO^{(+)}/SQ^-$. The intermediate DAS component (τ_2 = 2.2 ps) is similar to an average of the DAS of the other two components, as has been observed before for coumarin C343 on NiO.[9,35,36] Both charge separation and recombination are typically multiexponential (or nonexponential) processes for dyes on mesoporous semiconductors, and the τ_2 component most likely represents the slower part of charge separation together with the faster part of the recombination processes. The constant (τ > 10 ns) c_4 component has very small amplitude and represents the minor fraction of slower recombination seen out to 50 ns in the ns-laser experiments above.

The difference in extinction coefficient is large for squaraine (ca. 2.5×10^5 M^{-1} cm^{-1} at 640 nm) and its anion radical (ca. 2.5×10^4 M^{-1} cm^{-1} at 480 nm).[32] As the charge separation and recombination overlap in time, the full yield of SQ^- was not monitored. Nevertheless, it appears from the magnitude of ground state bleach and SQ^- absorption that even the initial charge separation yield is less than one, in spite of the ultrafast reaction of the SQ* excited state. It is possible that (partial) aggregation leads to some self-quenching effects and a reduction in charge separation yield, as has been observed for electron *injection* from similar squaraines on TiO_2.[38] We note that the dyad and triad showed much less aggregation effects in the absorption spectrum.

The results show almost complete charge recombination on a 10−200 ps time scale; a DSSC based on NiO/SQ is expected to yield a very small photocurrent, unless the redox couple regenerates the dye in a process that is faster than diffusion controlled (see below).

NiO/SQ-PMI. Exciting the SQ unit of SQ-PMI at 670 nm results in an initial spectrum (0.1 ps) that is attributable to the SQ* singlet excited state (Figure 6a). The spectra are similar to the results for NiO/SQ, when the differences in SQ-unit ground state spectra are taken into account. However, in NiO/SQ-PMI the spectrum rapidly develops and after ca. 1 ps shows positive bands around 550 nm and >730 nm along with the SQ ground state bleach. These features are in agreement with the SQ^+ radical cation, suggesting intramolecular charge separation (SQ^+-PMI^-). The corresponding PMI^- displays slight bleach around 500 nm, but its broad absorption band around 650 nm is obscured by the strong ground state bleach of the SQ unit.

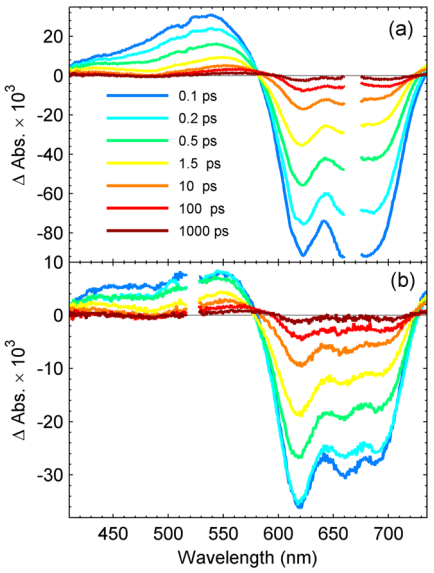

Figure 6. Transient absorption spectra of NiO/SQ-PMI excited at (a) 670 nm and (b) 523 nm. Samples as in Figure 3.

Table 2. Time Constants from Global Fits of Femtosecond TA Data[a]

	λ_{exc}/nm	τ_1/ps	τ_2/ps	τ_3/ps
NiO/SQ	647	0.45 (±0.15)	2.2 (±1.3)	53 (±73)
NiO/SQ-PMI	670	0.28 (±0.12)	3.0 (±4.1)	112 (±98)
	523	0.43 (±0.10)	5.5 (±2.4)	279 (±200)
NiO/SQ-PMI-NDI	670	0.21 (±0.1)	4.8 (±3.4)	130 (±74)
	523	0.29 (±0.21)	7.5 (±8.0)	166 (±182)
	400	0.19 (±0.14)	7.9 (±7.5)	164 (±298)

[a]Errors in parentheses are standard deviations which are obtained from local fit at all wavelengths.

dx.doi.org/10.1021/jp408900x | J. Phys. Chem. C 2014, 118, 103−113

The transient absorption then decreases in intensity, due to SQ^+-PMI^- recombination, with only minor changes in spectral shape during 1−1000 ps. Thus, hole injection into NiO to give the $NiO^{(+)}$/SQ-PMI^- state appears to occur mainly on the >1 ns time scale to give the clear PMI^- spectrum at 50 ns of Figure 3 above. However, the shifting isosbestic points around 575 and 720 nm between 10 and 1000 ps suggest that partial hole injection may already occur on this time scale. Due to intramolecular recombination in competition with hole injection, the overall signal decays to a large extent over this same time scale. When compared with the triad system (Figure 3), the lower yield of charge separation after 50 ns supports this conclusion. There is no clear sign of SQ^- from an initial interfacial charge separation, as in NiO/SQ, but we cannot exclude that this reaction occurs in parallel to some extent, presumably followed by electron shift to the PMI unit and therefore leading to the same product as for initial intramolecular charge separation.

Excitation of the PMI unit at 523 nm gave very similar spectra after 1.5 ps to those with 670 nm excitation (Figure 6b). However, the initial spectrum and the spectral evolution up to 1 ps were different from what is obtained with 670 nm excitation. The strong SQ unit bleach observed at 0.1 ps suggests ultrafast intramolecular charge separation, energy transfer, or a somewhat delocalized initial excited state. However, as the 0.1 ps spectrum is different from that obtained with 670 nm excitation and shows no stimulated emission, we believe the charge transfer process dominates. Note also that the ns experiments showed a higher charge separation yield with 523 nm than 670 nm excitation, which demonstrates that excitation of PMI must lead to charge separation that, at least to some extent, does not go via the SQ* singlet state.

NiO/PMI-NDI. This system was investigated in refs 3 and 14. Briefly, excitation of the PMI unit led to ultrafast hole injection ($t_{1/2} \approx 0.1$ ps) and a quantitative shift of the excess electron to the NDI ($t_{1/2} \approx 1$ ps), followed by recombination to the ground state on the 10−100 μs time scale.

NiO/SQ-PMI-NDI. Regardless of excitation wavelength, either 400, 523, or 670 nm, the spectrum after 0.1 ps shows a clear signature of the reduced NDI^- unit (peak at 480 nm) and strong SQ ground state bleach (Figure 7). A fit to the 480 nm traces shows a rise time of 0.2−0.3 ps (Figure S7 in the Supporting Information, Table 2), implying that intramolecular charge separation to give the NDI^- species was ultrafast for all excitation wavelengths. For 670 nm excitation, the spectrum after 0.1 ps shows features of the initial SQ* singlet excited state; excitation at 523 nm results in the 530 bleach and 570 absorption features of the PMI^+ species.[14] This PMI^+ feature then disappears on the 1−10 ps time scale while the NDI^- remains, which suggests a hole shift reaction to the SQ unit (the SQ^+ absorption around 480 nm cannot be distinguished below the NDI^- absorption). This charge separation pathway via the NDI^--PMI^+ state seems to dominate over primary electron transfer from SQ to the excited PMI*, forming the PMI^--SQ^+ state, as was the case for NiO/SQ-PMI.

It is clear that the SQ bleach initially grows after 523 nm excitation, and this is even clearer after 400 nm excitation. These observations are consistent with charge separation from the PMI* and NDI* excited states, and not with a delocalized excited state or primary excitation energy transfer to SQ*. For all excitation wavelengths the SQ bleach then disappears on a 10−1000 ps time scale while the NDI^- absorption at 480 nm remains relatively constant, consistent with hole injection from

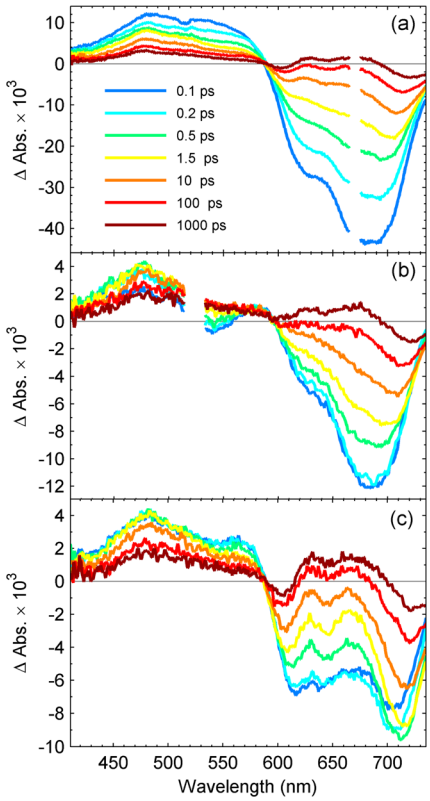

Figure 7. Transient absorption spectra of NiO/SQ-PMI-NDI excited at (a) 670 nm, (b) 523 nm, and (c) 400 nm. Samples as in Figure 3.

SQ^+ into NiO on this time scale. Importantly, there is no spectroscopic evidence for direct hole injection from either PMI* or NDI* to NiO, so alternative binding via other groups than the carboxylate, or with the molecule lying flat on the NiO surface, seems not to impact the data. The yield of hole injection into NiO appears to be ca. 40% for both 523 and 400 nm excitation, as estimated from the relative magnitudes of the initial (τ = 1.5 ps) and final (τ = 1000 ps) NDI- absorption at 480 nm; at 1000 ps, the SQ ground state bleach has disappeared and only the Stark signal remains, indicating that hole injection is completed. With SQ excitation at 655 nm, the initial hole injection yield is larger, as direct hole injection from SQ* competes with intermolecular charge separation. The former process, leads to relatively rapid recombination, however, as discussed above.

The lifetime components in Table 2 were acquired from a global fit according to eq 2. The DAS of the initial τ_1 component is very different depending on the excitation wavelengths (Figure S6, Supporting Information), and consistent with the local excited state of the unit excited. This is indicative that excitation energy transfer to the lower energy units does not dominate the dynamics, nor is the initial excited state completely delocalized.

The τ_3 component DAS shows the disappearance of the NDI^- absorption (480 nm), SQ^+ absorption (550 nm), and SQ bleach on the 150 ps time scale for all excitation wavelengths, consistent with hole transfer from SQ^+ to the NiO, in competition with intramolecular charge recombination. As for the dyad above, the τ_2 component DAS is a mixture of the τ_1 and τ_3 DAS, further emphasizing the multiexponential kinetics of these reactions. The c_4 component is already in good agreement with the 50 ns spectra of Figure 3, showing that the

dx.doi.org/10.1021/jp408900x | J. Phys. Chem. C 2014, 118, 103−113

fully charge separated state $NiO^{(+)}$/SQ-PMI-NDI^{-} is developed after ca. 1 ns.

SUMMARY OF TRANSIENT ABSORPTION RESULTS

An overall reaction scheme from the systems is given in Scheme 3, with approximate reaction lifetimes. In NiO/SQ, hole injection from the excited SQ into NiO occurs on a 0.45 ps time scale, but recombination is rapid, on the 10−200 ps time scale, leading to very little charge separation remaining on the >1 ns time scale. In NiO/SQ-PMI and NiO/SQ-PMI-NDI intramolecular charge separation occurs (0.2−0.3 ps) to give the SQ^{+} and PMI^{-} or NDI^{-} species, irrespective of which unit is excited. Subsequent hole injection from SQ^{+} into NiO occurs on the time scale of ca. 100 ps, in competition with intramolecular recombination. With direct excitation of the SQ unit, direct hole transfer to NiO presumably occurs in parallel to intramolecular charge separation, but this appears to give a lower yield of products surviving on the ns time scale than with excitation of the other units. Irrespective of which unit is excited, the yield of $NiO^{(+)}$/SQ-PMI-NDI^{-} at 50 ns is higher than of $NiO^{(+)}$/SQ-PMI^{-}, and much higher than that of $NiO^{(+)}$/SQ^{-}, showing that intramolecular recombination was slowed down by the localization of the electron further away from the SQ^{+} hole. Also the ultimate recombination with the $NiO^{(+)}$ was slower in the triad system ($\langle\tau\rangle$ = 26 μs) than for the dyad ($\langle\tau\rangle$ = 5 μs).

Photovoltaic study. The sensitizers were tested in NiO based DSSC devices using either the conventional triiodide/iodide electrolyte or the $cobalt^{III/II}$ electrolyte and the data are collected in Table 3.

Table 3. Photovoltaic Performances of the Sensitizers in NiO Solar Cells in Response to 100 mW/cm^2 Illumination

dye	redox couple	J_{SC} (mA cm^{-2})	V_{OC} (mV)	ff	η (%)
SQ	I_3^-/I^-	1.18	85	0.34	0.034
	$Co^{III/II}$	0.12	85	0.30	0.0041
PMI-NDI	I_3^-/I^-	0.69	135	0.35	0.033
	$Co^{III/II}$	1.06	315	0.31	0.10
SQ-PMI	I_3^-/I^-	1.31	65	0.31	0.026
	$Co^{III/II}$	0.34	95	0.28	0.009
SQ-PMI-NDI	I_3^-/I^-	2.73	95	0.32	0.083
	$Co^{III/II}$	1.17	175	0.27	0.055

Previous studies taught us that the triiodide/iodide electrolyte does not require a particularly long-lived charge separated state (NiO^{+}-S^{-}), but instead a relatively reducing sensitizer ($E_{1/2}$ (S/S^{-}) ≪ $E_{1/2}$(I_3^-/ $I_2^{\bullet-}$) = −0.5 V vs SCE). The cobalt electrolyte is easier to reduce ($E_{1/2}$ (Co^{III}/Co^{II}) = 0.1 V vs SCE), but is a slow electron acceptor owing to the large reorganization energy induced by the spin change when Co^{III} is converted to Co^{II}.[7,14,39] As a result, the reduced sensitizer (S^{-}) must be relatively long-lived (τ > 1 μs) to efficiently donate its electron to Co^{III} before the charge recombination takes place.

The photovoltaic measurements with the triiodide/iodide electrolyte showed that the short circuit photocurrent density steadily increases in the following order: SQ < SQ-PMI ≪ SQ-PMI-NDI (Table 3). Except PMI-NDI, whose particular case will be discussed below, the increase of the short-current density stems from the increase of larger light harvesting efficiency in agreement with the increasing number of chromophores in each system (Figure 8 and Table 3). This conclusion is well-supported by the photoaction spectra which show the production of electricity on all the absorption bands of each chromophore (Figure 9). This highlights the benefit of having a multichromophoric sensitizer to enlarge the photoactivity of the squaraine dye.

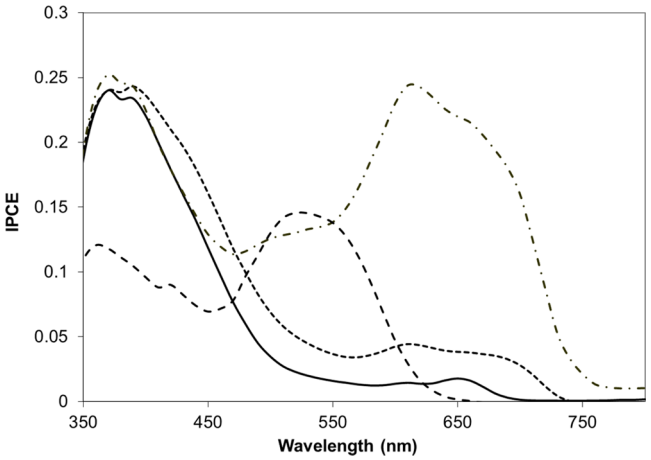

Figure 9. Photoaction spectra of the systems with the triiodide/iodide electrolyte. SQ, plain line; SQ-PMI, dotted line; SQ-PMI-NDI, dash-dot line; PMI-NDI, dashed line.

With the cobalt electrolyte, the plain squaraine (SQ) is not very active, because the reduced squaraine is too short-lived to reduce the electrolyte (see photophysical study above). In the dyads and the triad, the lifetime of the charge separated state is long (>5 μs) and we can therefore observe a significant

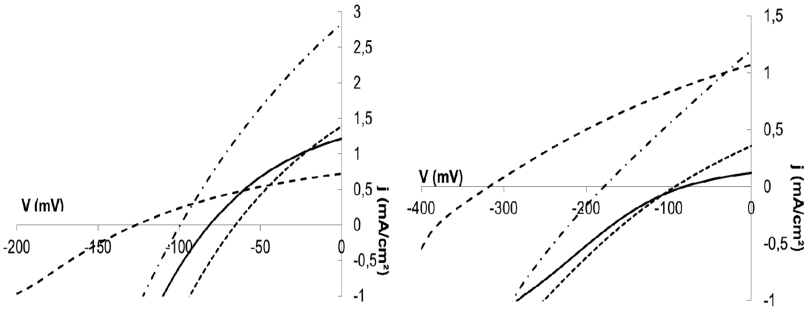

Figure 8. Current/voltage characteristics of the sensitizers in DSSC with the triiodide/iodide electrolyte (left) and cobalt electrolyte (right). SQ, plain line; SQ-PMI, dotted line; SQ-PMI-NDI, dash-dot line; PMI-NDI, dashed line. Measurements recorded in the dark are displayed in the Supporting Information.

dx.doi.org/10.1021/jp408900x | J. Phys. Chem. C 2014, 118, 103−113

photocurrent density and photovoltage compared to those measured with SQ. The dyad PMI-NDI, which is also a bichromophoric system, outperforms SQ-PMI since PMI-NDI exhibits higher photovoltage and larger photocurrent than SQ-PMI. However, the lifetimes of the charge separated state in SQ-PMI and SQ-PMI-NDI are particularly long and therefore their lower performances cannot be ascribed to an inefficient reduction of the electrolyte. The most plausible explanation comes from the operation mechanism, which is relatively different in SQ-PMI and SQ-PMI-NDI compared to that in PMI-NDI. Indeed, in PMI-NDI, the first charge separation event is the hole injection in NiO while in the former it is an intramolecular charge separation leading to SQ^+-PMI^-. The latter state can inject a hole into NiO valence band ($hinj_2$), but the intramolecular charge recombination (icr_1) being very fast due to the high electronic coupling between SQ and PMI, and therefore the overall quantum efficiency of the hole injection is reduced compare to that in PMI-NDI. Indeed, the quantum yield of NiO^+-PMI-NDI^- formation was previously estimated to be higher than 85%.[3] This operation mechanism also explains the much larger photocurrent measured with the triad over that of the dyad SQ-PMI. In the triad, the intramolecular electron shift reaction (esh_3) competes with the intramolecular charge recombination (icr) and this most certainly improves the quantum efficiency of the hole injection step ($hinj_3$). Indeed, the electron is moved on NDI further away from the squaraine limiting thus the intramolecular charge recombination between SQ^+ and PMI^-. Moreover, the squaraine dyes are known to be particularly prone to aggregation and this certainly decreases the overall efficiency owing to self-quenching process. As judged from the relative intensity of the absorption band of the aggregates at 600−640 nm on the spectra recorded on NiO, the degree of aggregation decreases in the following order: SQ > SQ-PMI ≫ SQ-PMI-NDI. The lower population of aggregates in the triad may certainly also contribute to the larger photocurrent measured than with the dyad SQ-PMI. Although the number of chromophores and the absorbance of the electrodes are quite similar with SQ-PMI and SQ-PMI-NDI (Figure 2), it is clearly seen on the photoaction spectrum that the IPCE is higher with SQ-PMI-NDI than that with SQ-PMI of the dyad (Figures 9 and 10).

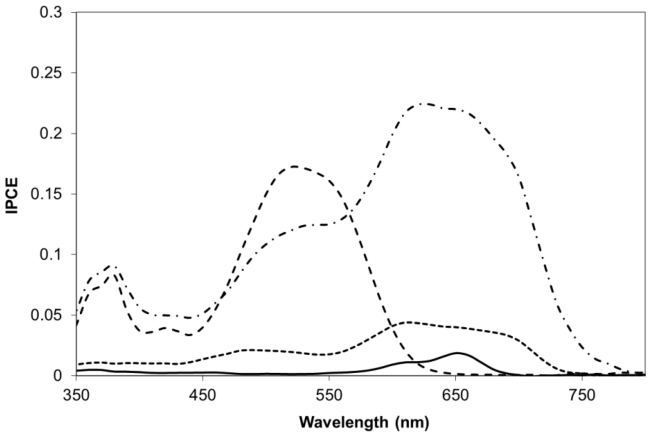

Figure 10. Photoaction spectra of the systems with the cobalt electrolyte. SQ, plain line; SQ-PMI, dotted line; SQ-PMI-NDI, dash-dot line; PMI-NDI, dashed line.

CONCLUSIONS

In this study, we designed, utilized, and characterized novel multichromophoric photosensitizer systems for NiO-based DSSCs that reproduce both the antenna effect and reduce the charge recombination rate by increasing the distance between the excess electron and NiO hole. In the new squaraine systems, a PMI antenna unit, which plays the dual role of light collector and secondary electron acceptor, is appended to the primary squaraine sensitizer.

First, it was observed that a simple squaraine dye could be an efficient sensitizer of NiO, since the hole injection is very fast and certainly reaches a unity quantum yield efficiency with the simple SQ dye. However, upon hole injection, the resulting excess electron density on the reduced SQ is not sufficiently spatially separated from the NiO surface to maintain a significant lifetime of the radical anion. The development of new and better performing squaraine based sensitizers will require engineering push−pull systems that contain an electron withdrawing group in the place of the iodo group. We are actively working in this direction.

The second piece of information concerns the importance of the operation mechanism for a multicomponent sensitizer on the overall photovoltaic performances. The presence of a secondary electron acceptor proximate to the squaraine sensitizer unit opens the possibility of a competing intramolecular electron transfer (steps 6 and 7, Scheme 1) over the desired hole injection from sensitizer excited-state (step 4, Scheme 1) or energy transfer from the antenna excited-state (step 3, Scheme 1). As a consequence, recombination of the resulting charge separated state (NiO-S^+-A^-) can outcompete the hole injection from the oxidized sensitizer and this importantly decreases the overall photovoltaic performances.[40] The control of the kinetics of this side-reaction (intramolecular electron transfer versus hole injection and energy transfer from the antenna) is therefore crucial and it can be achieved by a suitable choice of the spacer between the sensitizer and the antenna, which governs the distance and electronic coupling. In the compounds prepared herein, the lower photoconversion efficiency of the SQ-PMI and SQ-PMI-NDI compared to that of PMI-NDI mainly comes from a change of the photophysical operation mechanism. However, this study shows that the development of bichromophoric systems in which the antenna serves as both an electron acceptor and a photon harvester is a realistic strategy to boost the photovoltaic performances of a given sensitizer. This is demonstrated by the enhanced light-harvesting cross-section and much longer lived charge separated state with the dyad and the triad compared to the simple reference dye SQ. In engineering, future multi-chromophoric photosensitizers for p-type DSSCs it will be necessary to consider the design principles and results presented herein when creating the next generation of efficient photosensitizers.

ASSOCIATED CONTENT

Supporting Information

Calculation sof the free energy of the energy and electron transfer reactions, synthetic procedures for the preparation of the materials, fabrication of the solar cells and additional photovoltaic measurements, additional femtosecond transient absorption traces. This material is available free of charge via the Internet at http://pubs.acs.org.

dx.doi.org/10.1021/jp408900x | J. Phys. Chem. C 2014, 118, 103−113

AUTHOR INFORMATION

Corresponding Authors

*E-mail: Fabrice.Odobel@univ-nantes.fr. Fax: +33 251125402. Tel: +33 251125429.

*E-mail: Leif.Hammarstrom@kemi.uu.se. Fax: +46 18 471 6844. Tel: +46 18 471 3648.

Notes

The authors declare no competing financial interest.

ACKNOWLEDGMENTS

The authors wish to thank CNRS and the ANR HABISOL (program Asyscol, No. ANR-08-HABISOL-002) for financial supports and COST CM1202 programm (PERSPECT H2O). The Swedish Energy Agency, The K&A Wallenerg Foundation, and The Swedish Research Council (Contract 2009-4753) for financial support. J.G. would like to thank the Swedish Government's Strategic Research Area: STandUP for ENERGY.

REFERENCES

(1) Nakasa, A.; Usami, H.; Sumikura, S.; Hasegawa, S.; Koyama, T.; Suzuki, E. A High Voltage Dye-Sensitized Solar Cell Using a Nanoporous NiO Photocathode. *Chem. Lett.* **2005**, *34*, 500−501.

(2) He, J.; Lindström, H.; Hagfeldt, A.; Lindquist, S. E. Dye-Sensitized Nanostructured Tandem Cell - First Demonstrated Cell with a Dye-Sensitized Photocathode. *Sol. Energy Mater. Sol. Cells* **2000**, *62*, 265−273.

(3) Gibson, E. A.; Smeigh, A. L.; Pleux, L. L.; Fortage, J.; Boschloo, G.; Blart, E.; Pellegrin, Y.; Odobel, F.; Hagfeldt, A.; Hammarström, L. A p-Type NiO-based Dye-Sensitized Solar Cell with a Voc of 0.35 V. *Angew. Chem., Int. Ed.* **2009**, *48*, 4402−4405.

(4) Li, L.; Duan, L.; Wen, F.; Li, C.; Wang, M.; Hagfeldt, A.; Sun, L. Visible Light Driven Hydrogen Production From a Photo-Active Cathode Based on a Molecular Catalyst and Organic Dye-Sensitized p-Type Nanostructured NiO. *Chem. Commun.* **2012**, *48*, 988−990.

(5) Tong, L.; Iwase, A.; Nattestad, A.; Bach, U.; Weidelener, M.; Gotz, G.; Mishra, A.; Bauerle, P.; Amal, R.; Wallace, G. G.; Mozer, A. J. Sustained Solar Hydrogen Generation Using a Dye-Sensitised NiO Photocathode/$BiVO_4$ Tandem Photo-Electrochemical Device. *Energy Environ. Sci.* **2012**, *5*, 9472−9475.

(6) Odobel, F.; Le Pleux, L.; Pellegrin, Y.; Blart, E. New Photovoltaic Devices Based on the Sensitization of p-Type Semiconductors: Challenges and Opportunities. *Acc. Chem. Res.* **2010**, *43*, 1063−1071.

(7) Odobel, F.; Pellegrin, Y.; Gibson, E. A.; Hagfeldt, A.; Smeigh, A. L.; Hammarström, L. Recent Advances and Future Directions to Optimize the Performances of p-Type Dye-Sensitized Solar Cells. *Coord. Chem. Rev.* **2012**, *256*, 2414−2423.

(8) Borgström, M.; Blart, E.; Boschloo, G.; Mukhtar, E.; Hagfeldt, A.; Hammarström, L.; Odobel, F. Sensitized Hole Injection of Phosphorus Porphyrin into NiO: Toward New Photovoltaic Devices. *J. Phys. Chem. B* **2005**, *109*, 22928−22934.

(9) Morandeira, A.; Fortage, J.; Edvinsson, T.; Le Pleux, L.; Blart, E.; Boschloo, G.; Hagfeldt, A.; Hammarström, L.; Odobel, F. Improved Photon-to-Current Conversion Efficiency with a Nanoporous p-Type NiO Electrode by the Use of a Sensitizer-Acceptor Dyad. *J. Phys. Chem. C* **2008**, *112*, 1721−1728.

(10) Qin, P.; Wiberg, J.; Gibson, E. A.; Linder, M.; Li, L.; Brinck, T.; Hagfeldt, A.; Albinsson, B.; Sun, L. Synthesis and Mechanistic Studies of Organic Chromophores with Different Energy Levels for p-Type Dye-Sensitized Solar Cells. *J. Phys. Chem. C* **2010**, *114*, 4738−4748.

(11) Nattestad, A.; Mozer, A. J.; Fischer, M. K. R.; Cheng, Y. B.; Mishra, A.; Bäuerle, P.; Bach, U. Highly Efficient Photocathodes for Dye-Sensitized Tandem Solar Cells. *Nat. Mater.* **2010**, *9*, 31−35.

(12) Wu, X.; Yeow, E. K. L. Charge-Transfer Processes in Single CdSe/ZnS Quantum Dots with p-Ttype NiO Nanoparticles. *Chem. Commun.* **2010**, *46*, 4390−4392.

(13) Weidelener, M.; Mishra, A.; Nattestad, A.; Powar, S.; Mozer, A. J.; Mena-Osteritz, E.; Cheng, Y.-B.; Bach, U.; Bäuerle, P. Synthesis and Characterization of Perylene-Bithiophene-Triphenylamine Triads: Studies on the Effect of Alkyl-Substitution in p-Type NiO Based Photocathodes. *J. Mater. Chem.* **2012**, *22*, 7366−7379.

(14) Le Pleux, L.; Smeigh, A. L.; Gibson, E.; Pellegrin, Y.; Blart, E.; Boschloo, G.; Hagfeldt, A.; Hammarström, L.; Odobel, F. Synthesis, Photophysical and Photovoltaic Investigations of Acceptor-Functionalized Perylene Monoimide Dyes for Nickel Oxide p-Type Dye-Sensitized Solar Cells. *Energy Environ. Sci.* **2011**, *4*, 2075−2084.

(15) Qin, P.; Zhu, H.; Edvinsson, T.; Boschloo, G.; Hagfeldt, A.; Sun, L. Design of an Organic Chromophore for p-Type Dye-Sensitized Solar Cells. *J. Am. Chem. Soc.* **2008**, *130*, 8570−8571.

(16) Siegers, C.; Hohl-Ebinger, J.; Zimmermann, B.; Würfel, U.; Muelhaupt, R.; Hinsch, A.; Haag, R. A. Dyadic Sensitizer for Dye Solar Cells with High Energy-Transfer Efficiency in the Device. *ChemPhysChem* **2007**, *8*, 1548−1556.

(17) Lee, C. Y.; Hupp, J. T. Dye Sensitized Solar Cells: TiO_2 Sensitization with a Bodipy-Porphyrin Antenna System. *Langmuir* **2010**, *26*, 3760−3765.

(18) Tian, H.; Yang, X.; Pan, J.; Chen, R.; Liu, M.; Zhang, Q.; Hagfeldt, A.; Sun, L. A Triphenylamine Dye Model for the Study of Intramolecular Energy Transfer and Charge Transfer in Dye-Sensitized Solar Cells. *Adv. Funct. Mater.* **2008**, *18*, 3461−3468.

(19) Amadelli, R.; Argazzi, R.; Bignozzi, C. A.; Scandola, F. Design of Antenna-Sensitizer Polynuclear Complexes. Sensitization of Titanium Dioxide with $[Ru(bpy)_2(CN)_2]_2Ru(bpy(COO)_2)_2$. *J. Am. Chem. Soc.* **1990**, *112*, 7099−103.

(20) Warnan, J.; Buchet, F.; Pellegrin, Y.; Blart, E.; Odobel, F. Panchromatic Trichromophoric Sensitizer for Dye-Sensitized Solar Cells Using Antenna Effect. *Org. Lett.* **2011**, *13*, 3944−3947.

(21) Warnan, J.; Pellegrin, Y.; Blart, E.; Odobel, F. Supramolecular Light Harvesting Antenna to Enhance Absorption Cross-Section in Dye-Sensitized Solar Cells. *Chem. Commun.* **2012**, *48*, 675−677.

(22) Odobel, F.; Pellegrin, Y.; Warnan, J. Bio-Inspired Artificial Light-Harvesting Antennas to Enhance Solar Energy Capture in Dye-Sensitized Solar Cells. *Energy Environ. Sci.* **2013**, *6*, 2041−2052.

(23) McDermott, G.; Prince, S. M.; Freer, A. A.; Hawthornthwaite-Lawless, A. M.; Papiz, M. Z.; Cogdell, R. J.; Isaacs, N. W. Crystal Structure of an Integral Membrane Light-Harvesting Complex from Photosynthetic Bacteria. *Nature* **1995**, *374*, 517−521.

(24) Pullerits, T.; Sundström, V. Photosynthetic Light-Harvesting Pigment-Protein Complexes: Toward Understanding How and Why. *Acc. Chem. Res.* **1996**, *29*, 381−389.

(25) Odobel, F.; Zabri, H. Preparations and Characterizations of Bichromophoric Systems Composed of a Ruthenium Polypyridine Complex Connected to a Difluoroborazaindacene or a Zinc Phthalocyanine Chromophore. *Inorg. Chem.* **2005**, *44*, 5600−5611.

(26) Yum, J.-H.; Walter, P.; Huber, S.; Rentsch, D.; Geiger, T.; Nueesch, F.; De, A. F.; Graetzel, M.; Nazeeruddin, M. K. Efficient Far Red Sensitization of Nanocrystalline TiO_2 Films by an Unsymmetrical Squaraine Dye. *J. Am. Chem. Soc.* **2007**, *129*, 10320−10321.

(27) Geiger, T.; Kuster, S.; Yum, J.-H.; Moon, S.-J.; Nazeeruddin, M. K.; Grätzel, M.; Nüesch, F. Molecular Design of Unsymmetrical Squaraine Dyes for High Efficiency Conversion of Low Energy Photons into Electrons Using TiO_2 Nanocrystalline Films. *Adv. Mater.* **2009**, *19*, 2720−2727.

(28) Burke, A.; Schmidt-Mende, L.; Ito, S.; Grätzel, M. A Novel Blue Dye for Near-IR 'Dye-Sensitized' Solar Cell Applications. *Chem. Commun.* **2007**, 234−236.

(29) Chang, C.-H.; Chen, Y.-C.; Hsu, C.-Y.; Chou, H.-H.; Lin, J. T. Squaraine-Arylamine Sensitizers for Highly Efficient p-Type Dye-Sensitized Solar Cells. *Org. Lett.* **2012**, *14*, 4726−4729.

(30) Weil, T.; Abdalla, M. A.; Jatzke, C.; Hengstler, J.; Muellen, K. Water-Soluble Rylene Dyes as High-Performance Colorants for the Staining of Cells. *Biomacromolecules* **2005**, *6*, 68−79.

(31) Nolde, F.; Pisula, W.; Müller, S.; Kohl, C.; Muellen, K. Synthesis and Self-Organization of Core-Extended Perylene Tetracarboxdiimides with Branched Alkyl Substituents. *Chem. Mater.* **2006**, *18*, 3715−3725.

(32) Chen, J.; Winter, R. F. Studies on a Vinyl Ruthenium-Modified Squaraine Dye: Multiple Visible/Near-Infrared Absorbance Switching through Dye- and Substituent-Based Redox Processes. *Chem.—Eur. J.* **2012**, *18*, 10733−10741.
(33) Gosztola, D.; Niemczyk, M. P.; Svec, W.; Lukas, A. S.; Wasielewski, M. R. Excited Doublet States of Electrochemically Generated Aromatic Imide and Diimide Radical Anions. *J. Phys. Chem. A* **2000**, *104*, 6545−6551.
(34) Smeigh, A. L.; Pleux, L. L.; Fortage, J.; Pellegrin, Y.; Blart, E.; Odobel, F.; Hammarström, L. Ultrafast Recombination for NiO Sensitized with a Series of Perylene Imide Sensitizers Exhibiting Marcus Normal Behaviour. *Chem. Commun.* **2012**, *48*, 678−680.
(35) Morandeira, A.; Boschloo, G.; Hagfeldt, A.; Hammarström, L. Coumarin 343-NiO Films as Nanostructured Photocathodes in Dye-Sensitized Solar Cells: Ultrafast Electron Transfer, Effect of the I_3-/I- Redox Couple and Mechanism of Photocurrent Generation. *J. Phys. Chem. C* **2008**, *112*, 9530−9537.
(36) Morandeira, A.; Boschloo, G.; Hagfeldt, A.; Hammarström, L. Photoinduced Ultrafast Dynamics of Coumarin 343 Sensitized p-Type-Nanostructured NiO Films. *J. Phys. Chem. B* **2005**, *109*, 19403−19410.
(37) Freys, J. C.; Gardner, J. M.; D'Amario, L.; Brown, A. M.; Hammarström, L. Ru-based Donor-Acceptor Photosensitizer that Retards Charge Recombination in a p-Type Dye-Sensitized Solar Cells. *Dalton Trans.* **2012**, *41*, 13105−13111.
(38) de Miguel, G.; Marchena, M.; Ziółek, M.; Pandey, S. S.; Hayase, S.; Douhal, A. Femto- to Millisecond Photophysical Characterization of Indole-Based Squaraines Adsorbed on TiO_2 Nanoparticle Thin Films. *J. Phys. Chem. C* **2012**, *116*, 12137−12148.
(39) Gibson, E. A.; Smeigh, A. L.; Le Pleux, L.; Hammarström, L.; Odobel, F.; Boschloo, G.; Hagfeldt, A. Cobalt Polypyridyl-Based Electrolytes for p-Type Dye-Sensitized Solar Cells. *J. Phys. Chem. C* **2011**, *115*, 9772−9779.
(40) Chavhan, S. D.; Abellon, R. D.; van Breemen, A. J. J. M.; Koetse, M. M.; Sweelssen, J.; Savenije, T. J. Sensitization of p-type NiO Using n-type Conducting Polymers. *J. Phys. Chem. C* **2010**, *114*, 19496−19502.